FEB 28 1966

Method for Accelerating Flat Plates to High Velocity

A. S. Balchan amd G. R. Cowan

Reprinted from The Review of Scientific Instruments, Vol. 35, No. 8, pp. 937–944, August 1964

Reprinted from THE REVIEW OF SCIENTIFIC INSTRUMENTS, Vol. 35, No. 8, 937–944, August, 1964
Printed in U. S. A.

Method for Accelerating Flat Plates to High Velocity

A. S. BALCHAN AND G. R. COWAN
Eastern Laboratory, E. I. du Pont de Nemours & Company, Gibbstown, New Jersey
(Received 28 February 1964)

High velocity plates are useful in research, especially in the study of matter under high pressure. A scheme has been devised and tested for driving a thinner driven plate to a higher velocity than a driver plate of the same impedance. The increase is obtained in a collision process in which the driver strikes a buffer layer of lower impedance which is backed by the driven plate. The complex wave pattern has been examined in the acoustic approximation of constant impedance to obtain estimates of the optimum impedance ratios for several configurations which do not spall the driven plate. Experiments with head-on collisions observed by high speed photography and with oblique collisions observed by flash x radiography have demonstrated the technique in both single and multistage arrangements. The results agreed well with the acoustic approximation when the impedance ratio was evaluated at one-half of the pressure level obtained in the initial impact of driver against buffer. Photographic observation of the plate surface indicated substantially no breakup over a free run distance sufficient for the plate to reach terminal velocity.

INTRODUCTION

IN recent years, a great deal of interest has centered on the acceleration of metal bodies to very high velocities, particularly for the purpose of determining the possible effect of micrometeorite collisions on solid bodies. In addition, high velocity "driver" plates have been used[1–3] to generate shock waves having much higher pressure limits than are possible with direct impact by explosive detonation waves. Measurement of shock and material velocities enables the pressure and density to be determined. Experimentation in this country using the driver-plate technique has been done with high impedance drivers of about 2.5 mm thickness accelerated to velocities of about 5 mm/μsec by the use of cast high explosives. By allowing these drivers to strike a high impedance target material, a pressure close to 2 Mbar can be generated behind a shock wave which is constant in strength for a few microseconds, a time which is ample for measurement of the wave velocity. Workers in the Soviet Union have reported two series of higher pressure measurements on various metals (at about 5 and 10 Mbar) made using iron drivers (probably about 2.5 mm thick) at velocities of about 10.3 and 14.7 mm/μsec.

For driver plates placed on the surface of explosive charges, the maximum velocity that can be attained is the escape velocity of the detonation products, which Deal has shown[4] is approximately equal to the detonation velocity for certain high explosives when a plane detonation front reflects from a free surface at normal incidence. However data taken at this laboratory indicate that, at velocities in excess of about 3 mm/μsec, the efficiency of the explosive-driver systems (based on the fractional conversion of available energy to kinetic energy of the driver) falls rapidly.

This paper presents a method of accelerating a high impedance driver plate to a velocity theoretically in excess of that attainable with normal explosive-driver systems. The basis of the method is as follows: An initial high impedance driver (hereafter called "driver") is slowed by collision with a plate of lower impedance (hereafter called "buffer") to an interface velocity of greater than half of the initial plate velocity. When the shock in the buffer is

[1] R. G. McQueen and S. P. Marsh, J. Appl. Phys. **31**, 1253 (1960).
[2] L. V. Al'tshuler, K. K. Krupnikov, and M. I. Brazhnik, Zh. Eksperim. i Teor. Fiz. **34**, 886 (1958) [English transl.: Soviet Phys.—JETP **7**, 614 (1958)].
[3] L. V. Al'tshuler, K. K. Krupnikov, B. N. Ledenev, V. I. Zhuchikhin, and M. I. Brazhnik, Zh. Eksperim. i Teor. Fiz. **34**, 874 (1958) [English transl.: Soviet Phys.—JETP **7**, 606 (1958)].
[4] W. E. Deal, Third ONR Symposium on Detonation, Princeton University, 1960.

reflected from the opposite free surface, the free surface assumes a particle velocity of approximately twice the interface velocity. A thin, high impedance plate (hereafter called "driven plate") on this surface is accelerated by a series of shocks and rarefactions to this velocity, hence to greater than the velocity of the initial driver.

If the thickness of the driven plate is a moderate fraction of the thickness of the driver, the ultimate velocity of the driven plate will be reduced appreciably below the free surface velocity of the buffer, but may still significantly exceed the velocity of the driver plate. By using the driven plate of one stage as the driver plate of another stage, a multistage assembly can be set up to achieve progressively larger velocities.

THEORETICAL

Consider the case in which the driven plate is very thin compared to the driver and buffer plates, as illustrated schematically in Fig. 1. In this case a considerable number of reverberations of the initial shock transmitted into the driven plate can take place before any waves originating at the back surface of the driver or at the driver-buffer interface arrive at the driven plate.

The initial collision of driver and buffer produces shocks in both members. When the shock in the low impedance material reaches the interface with the driven plate, a shock is transmitted into the high impedance member and another reflected from the interface. The rarefaction from the free surface of the driven plate is transmitted through this interface as a rarefaction and reflected as a compressional disturbance. Both compressions and rarefactions in the driven plate add to the particle velocity of this plate in the direction of the driver motion, and the velocity of the driven plate asymptotically approaches the free surface velocity that would be attained by the buffer alone.[5]

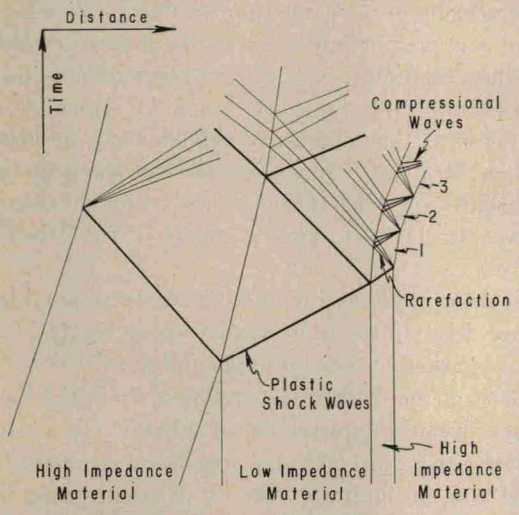


FIG. 1. Time-distance schematic diagram of the shock pattern to be expected when the driven plate is much thinner than the driver. The driver plate is on the left, the driven plate on the right. Shocks are shown as heavy lines, rarefactions as light lines.

It is seen that, if the driver velocity is V_1 and the particle velocity behind the initial shocks V', then for the thin driven plate under consideration, because of the difference in impedance,

$$V' > \tfrac{1}{2} V_1.$$

The free surface velocity of the buffer will be approximately $2V'$, while the velocity of the driven plate V_2 approaches $2V'$,

$$\lim V_2 = 2V' > V_1.$$

As an example of the simplified case (i.e., very thin driven plate) just described, a sample calculation was made of the particle velocity increase for several shock reverberations for the case of a stainless steel driver plate impacting a buffer of magnesium backed by a thin stainless steel plate, at a velocity of 4.95 mm/μsec, producing an initial impact pressure of 600 kbar.

For this approximate calculation, Hugoniot curves for magnesium and stainless steel were extrapolated using the linear shock velocity vs particle velocity relations obtained by Walsh *et al.*[6] and by Zukas.[7] The Hugoniot for the reflected wave in Mg above 600 kbar was assumed to be the same as the isentrope through the state behind the 600-kbar shock which was estimated by extrapolating the isentrope through $P=0$, $T=296$°C calculated by Walsh *et al.* and shifting it in a direction parallel to the volume axis. The isentrope for stainless steel was assumed to be the same as the Hugoniot curve. In the calculation it was assumed (as indicated in Fig. 1) that the "compressional" waves in the driven plate had built up into shocks by the time the waves reached the free surface of this plate.

TABLE I. Free surface velocities for sample case of shock configuration of Fig. 1.

	V_{fs}(mm/μsec)	$V_{fs}/V_{\text{initial}}$
Region 1	3.96	0.80
Region 2	5.67	1.15
Region 3	6.49	1.31
No final plate	7.66	1.55[a]
	7.87	1.57[b]

[a] If rarefaction particle velocity is 5% greater than shock particle velocity.
[b] If rarefaction particle velocity is 10% greater than shock particle velocity.

The calculated velocities for the regions designated in Fig. 1 are given in Table I.

It is seen that 3 shock reverberations are required to

[5] This statement is accurate only insofar as the reflected shock compression and subsequent rarefaction to the first shock pressure return the material to the same temperature as existed behind the initial shock.

[6] J. M. Walsh, M. H. Rice, R. G. McQueen, and F. L. Yarger, Phys. Rev. **108**, 196 (1957).

[7] E. G. Zukas (private communication to D. Warren, E.R.L., E. I. du Pont de Nemours & Company).

raise the particle velocity to 131% of the driver velocity. (The theoretical limit for this case probably lies between 155 and 157%.)

As the ratio of the thickness of the driver and buffer to the driven plate is reduced, the effects of the rarefaction centered at the rear surface of the driver, and the wave reflected from the driver-buffer interface, become important. In these cases, the shock diagram becomes more complicated. Since cases of practical interest are those in which the thickness of the driven plate is not very small compared to that of the driver, an effort was made in this work to establish a convenient method for predicting with reasonable accuracy the effect of the following parameters: (1) Ratio of thicknesses of high impedance members, (2) ratio of thickness of buffer to driver, and (3) ratio of impedances of buffer to driver (both high impedance members were assumed to be made of the same material).

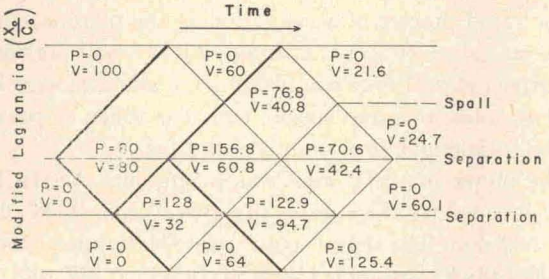


FIG. 2. "Acoustic approximation" solution for the case of a relatively thick driven plate (thickness ratio 2:1:1; impedance ratio 4:1). The driver is assigned an arbitrary velocity of 100. In the diagram, the order of layers, reading from top to bottom are high impedance driver, low impedance buffer, and high impedance driven plate. Shocks are shown as heavy lines, rarefactions as light lines. The solution for this case indicates a spall at the midpoint of the driver (see Figs. 5 and 6).

ACOUSTIC APPROXIMATION

In order to obtain some idea of how the relative thicknesses of driver, buffer, and driven plates, and the impedance ratio influence the velocity ratio, a series of calculations were made using an "acoustic approximation," which neglects the change of impedance with pressure. (Pressure and particle velocity were matched across interfaces; the equation $\Delta P = Z\Delta V$, where Z is the impedance, was used to relate the pressure change to the particle velocity change across a wave.) This proved useful as a guide in selecting values of the variables to be used in the experimental study designed to obtain conditions for optimum performance. As shown later, good agreement with experiment was obtained by the choice of an average impedance ratio computed at a pressure equal to one-half the pressure generated by the initial impact of driver against buffer.

Wave diagrams are most conveniently obtained in terms of a modified Lagrangian coordinate (S) defined as the initial (uncompressed) particle coordinate divided by the

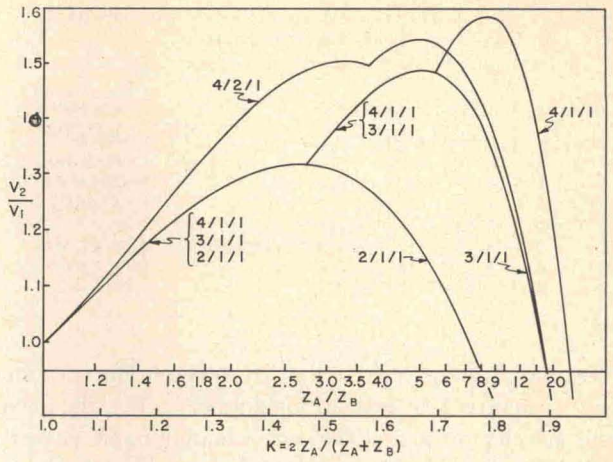


FIG. 3. Velocity ratio versus transmission coefficient for various plate thickness ratios obtained as analytic solutions to the "acoustic approximation."

wave velocity. A typical wave diagram is shown in Fig. 2. If the tensile strength of the material is insignificant, a condition which is approximated for very fast collisions, the wave diagram is terminated by a set of spalls which separate the plates into layers. For certain values of the thickness ratios (in terms of S), spalling of the driven plate does not occur, separation occurring at the interface between the buffer and driven plates. The predicted spalling of the driven plate may not actually occur, due to the finite strength of the material and the fact that the rarefaction waves spread considerably, thus reducing the tension in the driven plate before separation occurs at the interface. An average velocity of the driven plate can be obtained from the acoustic approximation by assuming that spalling does not occur.

For the special cases where no spalling of the driven plate is predicted, an expression for the velocity ratio (V_2/V_1) of the driven plate to driver plate can be obtained in terms of the pressure transmission coefficient K defined by $K=2Z_A/(Z_A+Z_B)$, where Z_A is the impedance of the driver and driven plates and Z_B is the impedance of the buffer. Figure 3 shows the velocity ratio for 2/1/1, 3/1/1, 4/1/1, and 4/2/1 configurations of S values of driver, buffer, and driven plates. It is to be noted that a higher velocity ratio is obtained for the 4/1/1 configuration compared to the 3/1/1 (and 3/1/1 compared to 2/1/1) only when the impedance ratio is sufficiently high. The 4/2/1 configuration gives a higher velocity ratio than the 4/1/1 configuration at low impedance ratios, but does not match the maximum velocity of the 4/1/1 reached at an impedance ratio of 8.39. For these configurations the expressions for velocity ratio are given in Table II.

A figure of merit for a configuration may be defined as $F=2\log(V_2/V_1)/\log(x_1/x_3)$, where x_1/x_3 is the ratio of driver to driven plate thickness. F has a maximum possible value of one when all of the kinetic energy of the

TABLE II. Analytic expressions for velocity ratios obtained from the acoustic approximation.

Configuration	Velocity ratio	Transmission coefficient K
2/1/1	$K(2-K)(K^2-K+1)$	$1<K<2$
3/1/1	$K(2-K)(K^2-K+1)$	$1<K<1.465$
	$K(2-K)(K^4-2K^3+2K^2-2K+2)$	$1.465<K<2$
4/1/1	$K(2-K)(K^2-K+1)$	$1<K<1.465$
	$K(2-K)(K^4-2K^3+2K^2-2K+2)$	$1.465<K<1.695$
	$K(2-K)(K^6-3K^5+4K^4-5K^3+6K^2-4K+2)$	$1.695<K<2$
4/2/1	$K(2-K)(2K^2-3K+2)$	$1<K<1.577$
	$K^2(2-K)(3K^2-7K+5)$	$1.577<K<2$

driver plate is transferred to the driven plate. The optimum impedance ratio (the ratio at maximum V_2/V_1), the maximum velocity ratio, and the corresponding figure of merit for the four configurations are shown in Table III.

These values are based on a purely one-dimensional analysis. In practice, edge effects will reduce the lateral dimensions of the portion of the driven plate which reaches maximum velocity below the dimensions of the driver plate.

EXPERIMENTAL

Experimental investigation of the plate acceleration scheme was done by two methods. The first utilized an oblique collision between the driver and buffer after a fixed amount of driver free-run. At a predetermined point in the collision, a flash radiograph was taken. Since a single observation of a steady-state oblique event is qualitatively similar to a one-dimensional time-distance plot (although the flow relations are different for plane and oblique collisions), measurement of the angles on the radiograph allowed calculation of the plate velocities. The second method employed a plane collision between driver and buffer assembly. The plates were silhouetted by a dim back-light and the cutoff of light caused by the moving plates recorded as an oblique trace on the film of a sweep camera.

Oblique Collision

The over-all experimental arrangement for the radiographic studies is illustrated schematically in Fig. 4. The driver in all cases was 1.6-mm-thick 304 stainless steel positioned at a predetermined angle from the buffer assembly. A plate of steel was used on the back of the explosive charge to give a higher velocity and to prevent spalling of the driver. The effect of edge lag of the initial

TABLE III. Optimum impedance ratio, maximum velocity ratio, and figure of merit for selected velocity ratios.

Configuration	Optimum Z_1/Z_2	Maximum V_2/V_1	$2\log(V_2/V_1)/\log(x_1/x_3)$
2/1/1	2.67	1.318	0.797
3/1/1	5.07	1.488	0.724
4/1/1	8.39	1.585	0.665
4/2/1	4.99	1.543	0.626

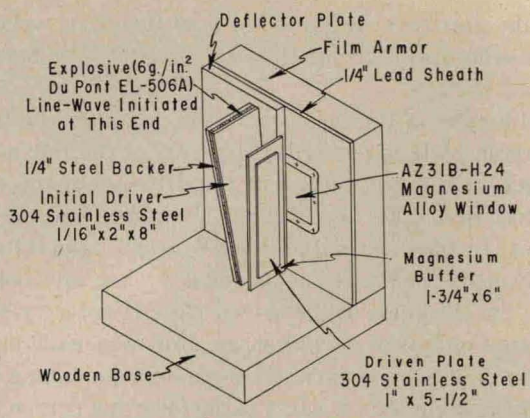


FIG. 4. Schematic diagram of the assembly employed in the radiographic studies. The subject is radiographed perpendicular to the magnesium "window."

driver was minimized by reducing the dimensions of the buffer relative to the initial driver, as illustrated. (Because of the rapid process of acceleration at the plate thickness used, lateral relief waves affected only a small portion of the driven plate.) Free run distances in all cases were held to close tolerances and special care was taken to prevent lateral misalignment of sample and driver.

The buffer material used was magnesium AZ31B-H24 alloy in nominal thicknesses of 0.406, 0.635, 0.787, 1.27, and 2.39 mm. The driven plate was 304 stainless steel in nominal thicknesses of 0.152, 0.305, 0.635, 0.787, and 1.27 mm. Intimate contact between buffer and final driver was obtained by applying a thin film of epoxy resin to one surface and pressing the assembly between surface ground steel plates at 2000 psi until the epoxy had set. The result was a joint which was approximately 0.005 mm thick and which withstood considerable handling.

The flash radiographic technique used was the same as previously described.[8] The film armor consisted of a lead-sheathed 1-in.-thick steel plate with a 1-×3-in. centered cutout through which the subject was viewed. A $\frac{1}{2}$-in.-thick AZ31B-H24 magnesium alloy "window" was set and bolted on $\frac{1}{2}$-in.-wide shoulders around the cutout portion. By the use of this arrangement, it was found possible to reduce the distance from sample to film to about $2\frac{1}{2}$ in.

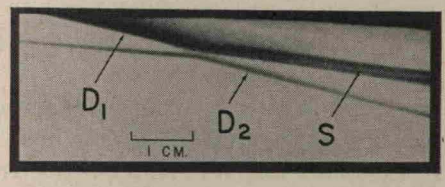


FIG. 5. Radiograph of oblique collision between driver (D_1) and buffer-driven plate (D_2) combination. Both driver and driven plate are 304 stainless steel and the buffer is magnesium alloy. (The buffer is partially obscured by small angle x-ray scatter). The thickness ratios in this case are 2:1:1 (see Fig. 2). Arrow S indicates a spall which separates the driver into two approximately equal segments as predicted by the acoustic method for this case (Fig. 2).

[8] A. S. Balchan, J. Appl. Phys. 34, 241 (1963).

and minimize scattering of the primary x-ray beam by the film armor. The tube-to-film distance was held at 195 in. The radiographic instrument was the model 506 tube and model 20100 pulser of the Field Emission Corporation. The tube was operated at 400 kV with a discharge time of 0.2 μsec.

In all experiments, the collision point was allowed to travel at least 75 mm before the radiograph was taken in order to minimize end effects. In this series, the explosive loading and the initial angle between driver and buffer were held constant.

Figures 5–8 illustrate typical radiographs for single and multiple (staged) collisions, with the conditions given for each case. (Positions of spall planes are indicated by S.)

For the case of two plates at an initial angle θ_i, when one (plate A) is driven through an angle γ into plate B by explosive with a detonation velocity D, the flow velocities

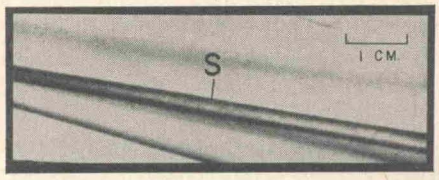


FIG. 6. Radiograph of the identical assembly as in Fig. 5 only viewed later in the acceleration process to illustrate the separation of the driver layers due to spall S.

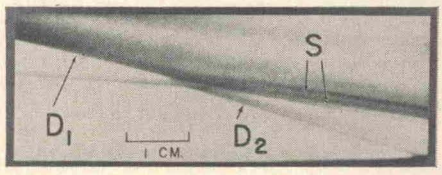


FIG. 7. Radiograph of oblique collision at thickness ratio 5.25:2.625:1 illustrating a double spall (S) in the driver.

of layers A and B into the collision point, relative to that point are given by

$$V_B = D \sin\gamma / \sin(\gamma - \theta_i),$$

$$V_A = [D \sin\gamma / \sin(\gamma - \theta_i)][\cos(\gamma/2 - \theta_i)/\cos(\gamma/2)].$$

(Note: If explosive is initiated at the "open" end of the initial angle, then θ_i will be positive.)

For small θ_i, V_B and V_A will be approximately equal.

It is seen that changes in both detonation velocity and initial angle between plates will effect the collision point velocity; since D was not measured on each shot, the knowledge of V_B was only as good as knowledge of the detonation velocity. The average measured value of V_B over the entire series of shots was 10.87 mm/μsec. At the pressure levels used in these experiments, this collision point velocity enabled the flow velocity behind all shocks to remain supersonic, ensuring steady flow at a reasonable distance from the end of the plate. (Although the values

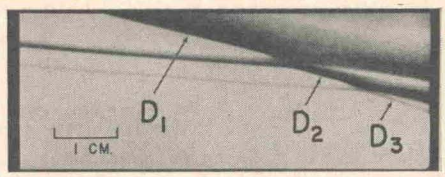


FIG. 8. Radiograph of "double collision" assembly. The initial driver D_1 accelerates an intermediate plate D_2 which becomes the driver for the second collision, accelerating plate D_3. The thickness ratios for the two stages are 2:1:1 and 2.625:1.313:1. Most of the final stage is again obscured by x-ray scatter.

calculated for each shot vary only from 10.52 to 11.13 mm/μsec, these numbers do not reflect variations in the detonation velocity.)

In any experiment, the radiograph enabled determination of the angle between driver and buffer at the collision point (θ_h), and the angle of the driven plate with respect to its initial position (θ_f). In addition, a preview radiograph was taken of each assembly to determine accurately the initial plate angle (θ_i). Since the angle γ is the sum of θ_h and θ_i, the plate velocities could be calculated from the formulas

$$V_1 = 2D \sin(\gamma/2),$$

$$V_2 = 2V_B \sin(\theta_f/2),$$

or

$$V_2/V_1 = [\sin(\theta_h+\theta_i) \sin(\theta_f/2)/\sin[(\theta_h+\theta_i)/2] \sin\theta_h],$$

where V_1 and V_2 are the velocities of plates A and B, respectively. It is seen that the quantity of interest (V_2/V_1) can be determined only from the angles θ_i, θ_h, and θ_f without knowledge of the detonation velocity.

A series of shots using magnesium alloy buffers was made for the single-collision case using the radiographic technique. The "smoothed" results are plotted in Fig. 9 as the velocity ratio versus the driver to driven plate

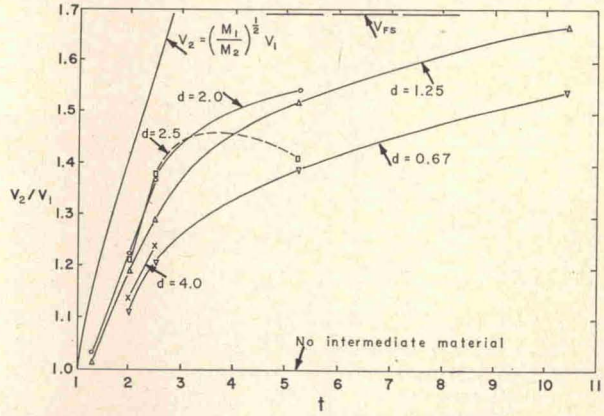


FIG. 9. Summary of oblique radiographic results. The velocity ratio V_2/V_1 is plotted as a function of the thickness ratio t of the high impedance driver and driven plate and d, the thickness ratio of the driver to the low impedance buffer. V_{FS} is the ratio of the magnesium buffer free surface velocity to the driver velocity. Each point is the average of at least two shots, and, at $d=2.0$ and 2.5, between 2 and 5 shots.

TABLE IV. Velocity ratios across double collision.

Experimental arrangement	Number of shots	Average over-all observed ratio	Over-all ratio predicted from individual values
Oblique collision $V_c \cong 10.87$ mm/μsec			
Driver 1.6-mm stainless steel			
First assembly { 0.787-mm magnesium alloy / 0.787-mm stainless steel	3	1.73	1.697
Second assembly { 0.406-mm magnesium alloy / 0.305-mm stainless steel			
Plane collision			
Average driver velocity 3.488 mm/μsec			
Driver 1.6-mm stainless steel			
First assembly { 0.787-mm magnesium alloy / 0.787-mm stainless steel	2	1.76	1.837
Second assembly { 0.406-mm magnesium alloy / 0.305-mm stainless steel			

(stainless steel) thickness ratio t and the driver to buffer thickness ratio d (using nominal thicknesses). The curve from the origin represents complete transfer of kinetic energy from the driver to the driven plate. At $d=2.0$ and $d=2.5$, each of the data points plotted represents the average of from 2 to 5 experiments, since these values of d represent nearly optimum values and more accurate data were desired. The actual curves through the data points should probably exhibit "bumps" because of the discontinuous nature of the acceleration process, but too few values of t were used to illustrate this effect.

In some cases the driver was observed to separate behind the collision point. In most cases the acoustic calculations indicated spalling in the driver (in some instances in more than one plane) and, at certain values of t, in the driven plate as well. Since the positions of the experimental spalls could not be determined with accuracy from the radiograph, no quantitative comparison of experimental spall planes with those predicted by the acoustic method could be made. In no case was spalling observed radiographically in the driven plate.

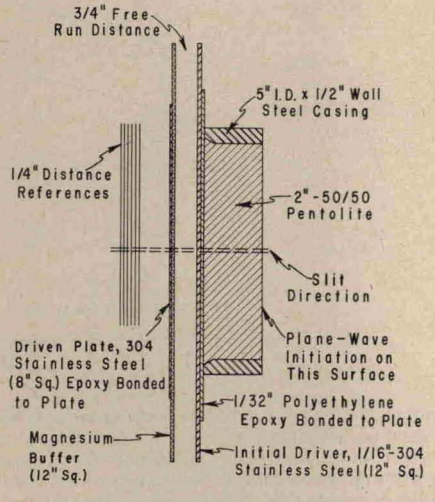


FIG. 10. Schematic cross-sectional illustration of the assembly used in the streak camera studies.

As a check on the velocity ratios across single collisions and on the possibility of spalling of the driven plate, experiments were run in which two stages of acceleration were used. The observed velocity ratios through the staged process and the values computed for the combination from the data of Fig. 9 are listed in Table IV. The relatively close agreement indicates that, at least for this particular value of t and d, and under the conditions of the experiment (i.e., oblique collision, relatively low driver velocity), no spalling of the "intermediate" driven plate occurred.

Plane Collision

The over-all plate arrangement in the streak camera studies is illustrated schematically in Fig. 10. Edge losses were minimized by encasing the charge in a $\frac{1}{2}$-in.-thick steel shell. The ends of the charge were planed smooth and the plate cemented under slight pressure to the charge. As in the case of the radiographic experiments, the driven plate was epoxy bonded under pressure to the buffer material; an 0.8-mm-thick layer of polyethylene was similarly bonded to the driver to prevent breakup of the plate during acceleration.

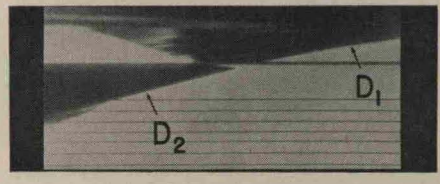


FIG. 11. Typical streak record of a single stage plane collision using 304 stainless steel driver and driven plates and magnesium alloy buffer. Arrow D_1 indicates the driver, arrow D_2 the driven plate. Time increases to the left.

All experiments carried out in this series were run in a vacuum of 5 mm Hg or less to allow the drivers to be visible behind the air shock.

The driver and plate assembly was silhouetted with a backlight used either in conjunction with a Fresnel lens or relatively far from the sample to obtain reasonble collimation of light; the cutoff of light was recorded with a streak camera run at an average streak speed of 3.2 mm/μsec. A certain amount of accuracy was sacrificed by virtue of the fact that an imperfectly collimated backlight was used.

The materials used in this study were identical to those used for the radiographic work. The initial driver was 1.6-mm-thick 304 stainless steel, the buffer 0.787-mm-thick AZ31B-H24 magnesium alloy, and the driven plates 0.305, 0.635, and 0.787-mm-thick 304 stainless steel. Because of the relative difficulty of the arrangements required, only one thickness of buffer was used, this being determined to be near optimum from the radiographic results.

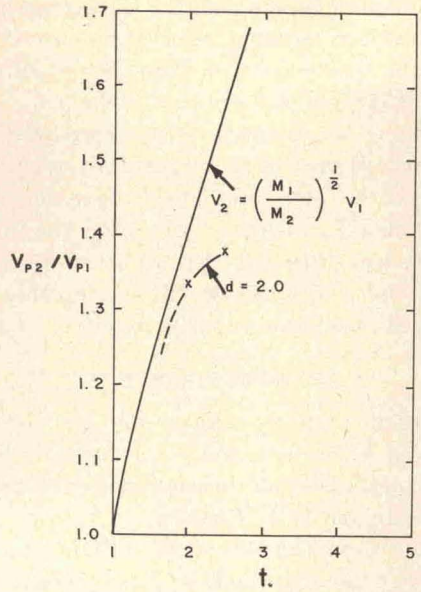


FIG. 12. Summary of plane collision, single stage results. All symbols have the same meaning as in Fig. 9. Each point represents the average of several experiments.

A typical streak camera record is shown in Fig. 11. Velocities were obtained from the slopes of the lines representing driver and driven plate motion. In general, the driven plate remained unbroken (at least in the slit plane) during a run of about 1.9 cm at approximately constant velocity; hence accurate velocities could be obtained. In contrast, the driver obviously underwent a certain amount of acceleration over the entire distance of free run (1.9 cm). A series of records such as that of Fig. 11, however, indicated no detectable acceleration (within the accuracy of the experiment) after a free run of 1.25 cm. Thus in all cases, the final 0.635 cm of travel was used for the measurement of the driver velocity. The driver velocity, measured in this manner, varied from 3.39 to 3.71 mm/μsec over the sequence of 15 shots.

The data obtained in this study are plotted in Fig. 12. These points represent the average of several experiments. At given t, the values of V_2/V_1 for the case of a plane collision lie somewhat above those in which the oblique collision was used.

Two "double-collision" shots were run in the plane configuration. The results (Table IV) indicated substantial agreement with the velocity ratio predicted from the individual values. An example of these shots is given in Fig. 13.

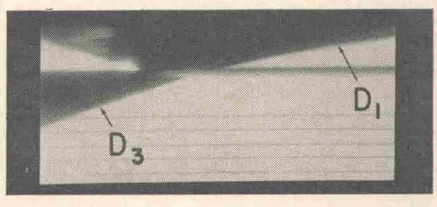


FIG. 13. Streak record of "double collision" plane assembly. The initial driver is D_1, the driven plate from the second state is D_3. Time increases to the left.

TABLE V. Comparison of experimental data with the results of the acoustic approximation. For oblique collision $P_1 = 164.4$ kbar, impedance ratio (Z) at average pressure of 82.2 kbar$\cong$3.84. For plane collision $P_1 = 367.2$ kbar, impedance ratio (Z) at average pressure of 183.6 kbar$\cong$3.57.

Driver:buffer:driven plate thickness ratio	Over-all velocity ratio from acoustic approximation $Z=3.0$	$Z=4.0$	Observed ratio oblique	plane
4/2/1	1.500	1.515	1.504	···
2/1/1	1.312	1.254	1.214	1.331
1.33/0.67/1	1.079	1.061	1.040	···

Comparison with Acoustic Approximation

In Table V are listed a series of calculations based on the acoustic approximation-velocity ratios for three thickness ratios at impedance ratios of 3 and 4. It is difficult to compare these values directly with those measured experimentally because of the variation of impedance ratios with pressure.

An approximate comparison of the calculated velocity ratios with those observed experimentally was made by assuming the average pressure through the acceleration process to be equal to one-half of the pressure generated by the initial collision. If the small difference between the acceleration process in the oblique and plane collision cases is neglected, then both processes could be compared to the results of the acoustic calculation as in the examples in Table V. [The difference between the modified (X/C_0) thickness ratios of the acoustic approximation and the real thickness (X) ratios used in the experimentation was neglected in this comparison.] The initial pressures were calculated from the previously quoted Hugoniot data for stainless steel and pure magnesium. Table VI indicates the effect of pressure on the impedance ratio of stainless steel and magnesium based on the Hugoniot data quoted previously (assuming the Hugoniot of pure magnesium to be identical to the alloy used). Agreement in all cases calculated was comparable to the illustrations in Table V.

TABLE VI. Ratio of shock impedances ($\rho_0 U_s$) of pure magnesium and stainless steel at high pressure (after data of Walsh *et al.*[6] and Zukas[7]).

Pressure (kbar)	$(\rho_0 U_s)_{SST}/(\rho_0 U_s)_{Mg}$
0 (weak plastic shock)	4.505
100	3.750
200	3.576
300	3.413
400	3.352

Observation of Plate Breakup

Several shots were made with a Beckman-Whitley model 189 framing camera to observe the outer surface of the driven plate in a typical plane collision assembly (1.6-mm stainless steel driver, 0.787-mm magnesium alloy buffer, 0.787-mm driven plate). The polished surface of the plate was used to reflect light from a 6-in.-diam argon flashlamp located 25 in. from the plate surface into the camera lens 170 in. from the plate. Irregularities in the plate surface appeared as dark patches. As the time and distance required for the driven plate to attain final velocity depend on the relative thicknesses, impedances, and pressure levels, it is necessary to determine these quantities in each individual case. The estimated distance required in the 2/1/1 configuration with impedance ratio of 3.5 and a driver plate velocity of 3.5 mm/μsec, based on a conservatively low value of the effective wave velocity of 5.5 mm/μsec, was found from the acoustic approximation to be not more than 0.87 times the thickness of the driven plate, i.e., about 0.69 mm, and the corresponding time required to achieve terminal velocity not more than 0.29 μsec. (In the double-collision plane shots, an interstage spacing of 0.787 mm was used, successfully.)

The framing sequences were not correlated with the start of outward motion of the plate. In no shot were irregularities of the plate noticed until the second frame after initial motion (i.e., at least 1 μsec after the initial plate motion). It was thus felt that sufficient planarity was maintained for a distance which considerably exceeded that required to achieve terminal velocity.

ACKNOWLEDGMENTS

The authors wish to acknowledge the assistance of R. E. Frie, J. E. Hudson, and J. C. Layton in the experimental arrangements and the continued encouragement of W. M. Branan and D. L. Coursen.

We should also like to thank W. E. Deal and members of the GMX-6 group at the Los Alamos Scientific Laboratory for their helpful suggestions.